Published in final edited form as:
Int J Cancer. 2012 March 1; 130(5): 1071–1081. doi:10.1002/ijc.26079.

D-4F, an apoA-I mimetic peptide, inhibits proliferation and tumorigenicity of epithelial ovarian cancer cells by upregulating the antioxidant enzyme MnSOD

Ekambaram Ganapathy[1], **Feng Su**[1], **David Meriwether**[1], **Asokan Devarajan**[2], **Victor Grijalva**[2], **Feng Gao**[1], **Arnab Chattopadhyay**[1], **G.M. Anantharamaiah**[3], **Mohamad Navab**[2], **Alan M. Fogelman**[2], **Srinivasa T. Reddy**[1,2,4], and **Robin Farias-Eisner**[1]

[1]Department of Obstetrics and Gynecology, David Geffen School of Medicine, University of California Los Angeles, Los Angeles, CA

[2]Department of Medicine, David Geffen School of Medicine, University of California Los Angeles, Los Angeles, CA

[3]Department of Medicine, University of Alabama at Birmingham, Birmingham, AL

[4]Department of Molecular and Medical Pharmacology, University of California Los Angeles, Los Angeles, CA

Abstract

We recently reported that apoA-I and apoA-I mimetic peptides prevent the development of flank tumors in immunocompetent C57BL/6J mice. To delineate the mechanism(s) of action of apoA-I mimetic peptides in tumor development, we examined the effect of D-4F (an apoA-I mimetic peptide) on the antioxidant status and on the gene expression and function of antioxidant enzymes in ID8 cells (a mouse epithelial ovarian cancer cell line) and in a mouse model. We demonstrate that D-4F treatment significantly reduces the viability and proliferation of ID8 cells, with a concomitant improvement of the antioxidant status of ID8 cells as measured by lipid peroxidation, protein carbonyl, superoxide anion, and hydrogen peroxide levels. D-4F treatment induces MnSOD (but not CuZnSOD) mRNA, protein, and activity. Inhibition of MnSOD in ID8 cells using shRNA vectors abrogates the inhibitory effects of D-4F on ID8 cell viability and proliferation. Moreover, tumor development from ID8 cells carrying shRNA for MnSOD were unaffected by D-4F treatment. Our results suggest that the inhibitory effects of D-4F on ID8 cell proliferation and tumor development are mediated, at least in part, by the induced expression and activity of MnSOD.

Keywords

MnSOD; apolipoprotein A-I; mimetic peptides; oxidative stress; animal models; epithelial ovarian cancer

Correspondence to: Robin Farias-Eisner, Department of OB/GYN, University of California Los Angeles, 650 Charles E. Young Drive South, CHS 24-127, Los Angeles, CA 90095, USA, Tel.: 310-794-1919, Fax: +310-206-3670, rfeisner@mednet.ucla.edu; or Srinivasa T. Reddy, Department of OB/GYN, Medicine, and Molecular and Medical Pharmacology, University of California Los Angeles, 650 Charles E. Young Drive South, MRL 3736 Los Angeles, CA 90095, USA, Te l.: 310-206-3915, Fax: +310-206-3605, sreddy@mednet.ucla.edu.

Additional Supporting Information may be found in the online version of this article.

Epithelial ovarian cancer (EOC) is the most lethal form of gynecological cancer worldwide. Despite excellent responses to early surgical and chemotherapeutic interventions, most of the affected individuals present with advanced disease.[1] The National Cancer Institute's 2010 estimate projects 21,880 new cases of EOC in the US. Advanced ovarian cancers are difficult to treat with the currently available chemotherapeutic regimen. Therefore, novel methods of therapy devoid of side effects are needed.

We previously identified three serum biomarkers—apolipoprotein A-I (apoA-I), transthyretin and transferin—that together with CA125 diagnose early-stage ovarian cancer.[2–4] We recently began exploring the role of apoA-I and apoA-I mimetic peptides for use as a therapeutic modality against ovarian cancer in preclinical studies.[5] ApoA-I mimetic peptides mimic the structural and functional properties of apoA-I and have been found to have significant therapeutic potential in various inflammatory diseases in both mice and primate models,[6,7] and in cardiovascular human patients.[8,9] Recently, we have shown that D-4F, one of the potent apoA-I mimetic peptides, retards the development of tumors in an animal model of ovarian cancer.[5] Although D-4F inhibits both cell viability and proliferation in cell culture models, the mechanism of action remains unknown.

In addition to the number of acquired genetic alterations in oncogenes and tumor suppressor genes (such as BRCA1, p53, MnSOD, nm23 and K-ras), EOC has consistently been associated with inflammation and oxidative stress.[10] Oxidative stress has been implicated in cell proliferation and malignant conversion during the development of ovarian cancer.[11] Elevated oxidative stress and free oxygen radicals have been associated with the increased risk of various cancers and end products of lipid peroxidation have also been suggested to play a role in tumorigenesis.[12,13] It has been shown previously that apoA-I can restore the balance between nitric oxide (NO) and superoxide (O_2^-) anions in mice,[14] indicating an antioxidant effect from the administration of apoA-I. Moreover, recent studies suggest that one of the mechanisms of action of apoA-I mimetic peptides is binding[15] and removal[16] of oxidized lipids from the circulation, thus reducing the oxidative stress.

The objective of our study was to determine the mechanism by which D-4F inhibits cell proliferation and viability in cancer cells and tumor growth *in vivo*. We show that, (*i*) D-4F improves the antioxidant status in ID8 cells, a mouse ovarian cancer cell line; (*ii*) inhibition of ID8 cell proliferation by D-4F requires the upregulation of MnSOD protein and activity and (*iii*) inhibition of MnSOD by shRNA reverses the effects of D-4F *in vivo*. Our results suggest that the antitumorigenic properties of apoA-I mimetic peptides are mediated, in part, by both a direct reduction in the oxidative stress and a simultaneous induction of MnSOD.

Material and Methods

Reagents and cell culture

ID8 cells were cultured in DMEM (high glucose) (Invitrogen, CA) supplemented with 4% fetal bovine serum (Sigma chemical, St. Louis, MO), 100 units/ml penicillin, 100 μg/ml streptomycin, 5 μg/ml insulin, 5 μg/ml transferrin and 5 ng/ml sodium selenite (Invitrogen, CA). Cultures were incubated at 37°C in 5% CO_2. Medium was changed every day. Cells were subcultured using 0.25% trypsin and 0.1% EDTA. The shID8 and shSOD2ID8 cell lines were established with control shRNA and MnSOD shRNA, respectively. Puromycin (1 μg/ml) was used for selection and maintenance of stable cell lines. The control shRNA and MnSOD shRNA were obtained from Open Biosystems, (Huntsville, AL). For all experiments, ID8, shID8 and shSOD2ID8 cells were switched to serum free media (overnight) prior experimental procedures. D-4F was used at 1 or 10 μg/ml (from 1000× stocks prepared in water).

Cell viability assay

3-(4,5-dimethylthiazol-2-yl)-5-(3-carboxymethoxyphenyl)-2-(4-sulfophenyl)-2H-tetrazolium (MTS) assay, an index of cell viability and cell growth, is based on the ability of viable cells to reduce MTS from a water-soluble dye to insoluble formazan product. The ID8 cells treated in the presence or absence of D-4F were seeded in 96 well plates at a density of 2×10^3 per well and mixed with 20 μl of MTS dye, and then incubated for 30 min in the dark. The optical density (OD) values were measured at 490 nm using BMG labtech plate reader (CA). For determination of cell viability, the relative cell viability (%) was calculated as [OD of treated sample × 100/control OD].

Cell proliferation assay

Cell proliferation was determined by measuring the incorporation of the pyrimidine analogue, 5-bromo-2′-deoxyuridine (BrdU; Roche Applied Science, IN) during DNA synthesis. Briefly, cells (2×10^3/well) were plated into 96-well flat bottom plates (Corning Incorporated, New York, NY) and allowed to attach overnight then acclimated to serum free medium conditions for 24 hrs. The ID8 cells were then treated with D-4F for 1, 2, 4, 22 or 46 hrs in serum free media. After the initital incubation with D-4F, BrdU (10 μM) was also added to the cells for an additional 2 hrs; cells were fixed and incubated for 2 hrs at 37°C with an anti-BrdU antibody-peroxidase conjugate. Immunocomplexes were detected by addition of a tetramethyl-benzidine (TMB) substrate solution according to the manufacturer's recommendations. The reaction was stopped by adding 50 μl of 0.5 M sulfuric acid, and the absorbance was measured with a plate reader (BMG Labtech, CA) at 450 nm. Experiments were performed in triplicates; data are expressed as the mean of the triplicate determinations (mean ± SD).

Measurement of extracellular hydrogen peroxide

Extracellular hydrogen peroxide (H_2O_2) was determined using the Amplex Red Hydrogen Peroxide Assay Kit (Invitrogen, CA) according to the manufacturer's protocol using a fluorescence spectrophotometer with a temperature-regulated chamber equipped with constant stirring. Amplex Red reacts with H_2O_2 to produce a fluorescent signal, measured at excitation and emission wavelengths of 560 and 590 nm, respectively. Briefly, add 20 μl of ID8 cells (2×10^4/well) were plated into 96-well flat bottom plates (Corning Incorporated, New York, NY) and allowed to attach overnight. After incubation with D-4F, 100 μl reaction mixture containing 50 μM Amplex® Red reagent, 0.1 U/ml horseradish peroxidase (HRP) in Krebs–Ringer Phosphate Glucose buffer (KRPG) and an activator of phorbol 12-myristate 13-acetate, was added. The KRPG consists of 145 mM NaCl, 5.7 mM sodium phosphate, 4.86 mM KCl, 0.54 mM $CaCl_2$, 1.22 mM $MgSO_4$, 5.5 mM glucose, pH 7.35. For negative control 20 μl of KRPG buffer without cells was added to 100 μl reaction mixture. After incubation of D-4F, Amplex Red conversion to resorufin was measured at stated above using a (Biotek Synergy-2, Vermont and USA) plate reader at wavelengths of excitation in the range of 540 nm and emission at 590 nm. Fluorescence was continuously measured and selected time points were recorded.

Dihydroethidium (DHE) assay

This assay is designed to measure dihydroethidium, which reflects the levels of superoxide.[17] ID8 cells were grown in 6-well plates, starved overnight in serum free media, and treated with D-4F for 1, 4 or 24 hrs. The cultures were washed twice with PBS and then stained for 30 min at 37°C with 10 μM dihydroethidium. The cells were washed twice with PBS and fluorescence was measured using a BMG lab-tech plate reader (CA) at wavelengths 485/585 nm. Each data point was performed in triplicate, and the results were reported as mean ± SD.

Measurement of total and oxidized glutathione

Intracellular levels of Glutathione (GSH) were determined by spectrophotometer using 5,5′-dithiobis-2-nitrobenzoic acid (DTNB) (Cayman Chemical, Ann Arbor, MI) which produces a yellow color with GSH to yield 5-thio-2-nitrobenzoic acid (TNBA). ID8 cells were plated in 60 mm dish (2×10^5 cells). After treatment with D-4F, the cells were trypsinized and pellet was collected. The cells were homogenized with ice cold 50 mM phosphate buffer (pH 7.0) containing 1 mM EDTA, centrifuged at 10,000*g* for 15 min at 4°C. Triethanolamine was added to the supernatants, adjusted to neutral pH, and DTNB reagent was added. The resulting solutions were measured at 405 nm in a BMG labtech plate reader (CA). The concentration of GSH was determined from a standard curve prepared with known concentrations of GSH under similar conditions and normalized using equal amounts of protein. GSH/GSSG ratio: ID8 (2×10^5) cells were treated with D-4F obtained by scraping off the bottom of the dish with a cell scraper. The cell pellets were once washed with ice-cold PBS, resuspended in lysis buffer (50 mM HEPES, pH 7.5, 10% sucrose, 0.1% Triton X-100), and placed on ice for 30 min. The supernatants were collected by centrifugation at 10,000*g* for 10 min. Oxidized glutathione (GSSG) levels were measured by masking the reduced glutathione (GSH) with 2-vinylpyridine. GSH/GSSG ratio was plotted according to the manufacturer's instructions in (Cayman Chemicals, Ann Arbor, MI) the assay kit. Each data point was performed in triplicate, and the results were reported as mean ± SD.

Assay of TBARS

Aldehydes such as malondialdehyde (MDA) and 4-hydroxy-nonenal (HNE) are formed during lipid peroxidation (LPO). The concentration of MDA was measured using the Cayman Chemicals TBARS assay kit. Briefly, 2×10^6 cells were cultured in 100 mm dish and treated with D-4F for 24 hrs. The cells were collected by scraping in 10 mM Tris-HCl buffer, pH 7.4, containing 0.125 M KCl, followed by low-speed centrifugation (10 min at 300*g*), resuspended in 0.5 ml of Tris-HCl, pH 7.4, and lysed using a sonicator for 5 sec on ice. An equal amount of protein in 200 μl aliquots from cell lysates was assayed for MDA according to the manufacturer's protocol.

Protein carbonyls content

Reactive oxygen species (ROS) are produced as a consequence of normal aerobic metabolism. The most general indicator and by far the most commonly used marker of protein oxidation is protein carbonyl content. The Cayman chemicals assay kit exploits the reaction between 2,4 dinitrophenylhydrazine (DNPH) and protein carbonyls. DNPH reacts with protein carbonyls, forming a Schiff base to produce the corresponding hydrazone, which can be analyzed spectrophotometrically at an absorbance between 360 and 385 nm, and the carbonyl content, can then be standardized to protein concentration. 1×10^5 cells were seeded into six well plates and after incubation of D-4F, cells were washed with PBS and lysed with ice cold 50 mM phosphate buffer at pH 6.7 containing 1 mM EDTA. After centrifugation at 10,000*g* for 15 min at 4°C, the supernant was removed and assayed for protein carbonyl content according to manufacturer's protocol.

SOD activity assay

ID8 cells treated or untreated with D-4F were harvested and lysed in 10 mM Tris/HCl, pH 7.4, containing 0.1% (w/v) Triton X-100. After centrifugation at 12,000*g* for 15 min at 4°C, lysates were treated with 1 mM KCN to inhibit CuZn-SOD before measuring MnSOD activity. MnSOD activity was measured in the supernatants using a kit from Cayman Chemicals (Ann Arbor, MI).

Western blotting

Cells in 6-well plate were rinsed with PBS and lysed in buffer containing 0.1 M NaCl, 5 mM EDTA, 50 μM sodium orthovanadate, 1% Triton X-100, and protease inhibitor tablet (Roche Diagnostics) in 50 mM Tris buffer (pH 7.5). The cell lysate (25 μg of protein/well) was loaded onto 12% SDS gel, transferred to nitrocellulose membrane, and incubated overnight at 4°C in 5% skim milk and 0.1% Tween-20 to block nonspecific binding. Membranes were then incubated with anti-MnSOD rabbit polyclonal antibodies or anti-CuZnSOD goat polyclonal antibodies (Abcam, MA) followed by incubation in anti-rabbit or anti goat secondary antibodies conjugated with horseradish peroxidase (1 hr, room temperature, 1:5000), respectively. Immunoreactive protein bands were visualized using the enhanced chemiluminescence detection system (Millipore, Billerica, MA). Protein loading was verified by stripping and reprobing blots with antibodies against β-actin.

Quantitative real time PCR analysis (qRT-PCR)

Total RNA was isolated from both treated and untreated ID8 cells using Qiagen RNA isolation kit. Real time PCR assay was done using SYBR Green PCR Master mix (Bio-Rad CFX-96 real time system) and PCR amplification was done using a Bio-Rad thermal cycler using the absolute quantification method. The cycling conditions were as follows: 3 min at 95°C followed by 40 cycles of: 95°C, 30 s; 60°C, 1 min; 72°C, 1 min; followed by a final extension at 72°C for 10 min. The primer pairs were as follows: MnSOD, (forward) 5′-CCTCAACGTCACCGAGGAGAAG-3′ and (reverse) 5′-CTCCCAGTTGATTACATTAGT-3′; cyclophilin used as an internal control (forward) 5′-GGCCGATGACGAGCCC-3′ and (reverse) 5′-TGTCTTTGGAACTTTGTCTGCAA-3′.

Generation of flank tumors in C57BL/6J mice

Six-week-old female C57BL/6J (Jackson laboratories) mice were maintained in a pathogen-free animal facility at least one week before use. All experiments were done in accordance with institutional guidelines. The mice were housed in a 12–12 hrs light–dark schedule and provided food and water *ad libitum.* The shSOD2ID8 or shID8 cells (5×10^6/mice) were injected subcutaneously in the right flank of C57BL/6J ($n = 15$ per group), and the peptide (D-4F, 300 μg/ml) was given in the drinking water for 5 weeks after the first day of cell injection. At the end of the 5th week, mice were sacrificed and tumors were resected. Tumor volume was determined by Vernier caliper and using a formula ($1/2 \times L \times W^2$) mm^3. The experimental groups were: shID8 cells alone (control); shID8 cells + D-4F (300 μg/ml in drinking water); shSOD2ID8 cells alone (control); shSOD2ID8 cells + D-4F (300 μg/ml in drinking water).

Statistical analysis

Data was expressed as mean ± SD where indicated. Statistical differences were analyzed using the Student's *t*-test and *p* values less than 0.05 were considered statistically significant.

Results

D-4F inhibits cell viability and cell proliferation in ID8 cells

We recently reported that apoA-I and the apoA-I mimetic peptides D-4F, L-4F and L-5F all inhibit ID8 cell proliferation and reduce tumor growth in a C57BL/6J mouse model of ovarian cancer.[5,18] To determine the mechanism by which D-4F inhibits ID8 cell proliferation and reduces tumor growth, we first examined the effect of D-4F on ID8 cell viability and cell proliferation *in vitro*. D-4F treatment (1 or 10 μg/ml) significantly reduced the number of viable ID8 cells (Fig. 1*a*). To further evaluate whether the reduced number of cells was due to an inhibition of proliferation, we examined the effect of D-4F on the

proliferation of ID8 cells in a BrdU incorporation assay. ID8 cells were grown to 50% confluence in 96 well plates and then starved for 24 hrs in serum free media. The ID8 cells were then treated with 1 μg/ml D-4F for various lengths of time, from 0 to 48 hrs. BrdU incorporation was measured across 46 to 48 hrs in every case. A significant reduction of ID8 cell proliferation was observed starting at 4 hrs after D-4F treatment (Fig. 1*b*). Moreover, D-4F did not cause detectable toxicity, apoptosis and autophagy at the concentrations used (Supporting Information Fig. 1).

D-4F reduces cellular oxidative stress in ID8 cells

Recent studies suggest that one of the mechanisms of action of apoA-I mimetic peptides is to reduce oxidative stress. To determine whether D-4F treatment affects superoxide generation, ID8 cells were incubated with or without D-4F for various time periods and analyzed for superoxide levels using DHE. Control cells exhibited significantly greater fluorescence intensity than D-4F treated cells, indicating that D-4F treated cells have significantly lower levels of superoxide (Fig. 2*a*). Since superoxide levels are reflected in H_2O_2 levels down-stream, we measured extracellular H_2O_2 levels in D-4F-treated ID8 cells using the Amplex Red reagent. ID8 cells that had been treated with D-4F (1 or 10 μg/ml) showed significantly lower H_2O_2 levels (Fig. 2*b*). As D-4F neither quenches Amplex Red directly, nor interferes with H_2O_2 and Amplex Red (data not shown), the results of the Amplex Red assay suggest that D-4F suppresses the production of H_2O_2. The presence of carbonyl groups on proteins is a widely accepted measure of oxidative damage of proteins under conditions of oxidative stress. We analyzed protein carbonyl content by measuring hydrazones in the presence of DNPH. As shown in Figure 2*c*, 4 and 24 hrs after D-4F treatment there was a significant decrease in protein carbonyl content in D-4F treated ID8 cells when compared to untreated cells. Lipid peroxidation is an important outcome of oxidative stress and we observed that D-4F treatment significantly reduced lipid peroxides in ID8 cells as measured by a TBARS assay (Fig. 2*d*). Moreover, as shown in Figure 2*e*, the GSH/GSSG ratio was markedly increased in D-4F-treated ID8 cells when compared to vehicle controls, suggesting that D-4F treatment elicits an overall reduction of oxidative stress in ID8 cells.

D-4F treatment increases MnSOD expression and activity in ID8 cells

We next examined whether decreased superoxide levels in D-4F treated ID8 cells are due to increased expression of the antioxidant enzymes CuZnSOD and MnSOD. D-4F did not cause changes in CuZnSOD protein expression. However, MnSOD protein expression was significantly increased in D-4F treated ID8 cells (Fig. 3*b*). Furthermore, we observed significant increases in both MnSOD mRNA expression and protein activity in D-4F treated ID8 cells when compared to untreated cells (Figs. 3*a* and 3*c*). These results suggest that MnSOD may play an important role in D-4F mediated reduction of oxidative stress and inhibition of cell proliferation in ID8 cells.

D-4F-mediated inhibition of ID8 cell proliferation requires the activity of MnSOD

We next examined whether MnSOD activity and function plays a role in the D-4F induced inhibition of cell proliferation. We established a stable ID8 cell line in which MnSOD was knocked down *via* a shRNA mechanism. We treated shID8 (control vector carrying ID8 cell line) and shSOD2ID8 (ID8 cell line stably expressing MnSOD shRNA) cells with D-4F peptide and measured cell viability, cell proliferation and protein activity (Figs. 4*a*, 4*b* and 4*d*). D-4F treated shID8 cells exhibited a significant reduction in viability and proliferation compared to untreated shID8 cells. In contrast, there was no difference in viability and proliferation of shSO-D2ID8 cells in the presence or absence of D-4F treatment. These results indicate that MnSOD mediates the inhibition of ID8 cell viability and proliferation that is effected by D-4F.

D-4F-mediated inhibition of tumor development is abrogated in the absence of MnSOD

Having demonstrated that D-4F inhibits ID8 cell proliferation *in vitro* through a MnSOD-mediated mechansim, we next examined whether the antitumorigenic effects of D-4F *in vivo*[5,18] are also modulated by MnSOD levels. We studied the ability of D-4F peptide to inhibit tumor development in a mouse model of ovarian cancer as reported previously.[5] The shID8 and shSOD2ID8 cells were subcutaneously injected into the right flanks of C57BL/6J mice (n = 30 per cell line), and D-4F or vehicle were administered in drinking water (300 μg/ml) to half of the mice in each group (n = 15). As reported previously,[5] D-4F treatment significantly reduced the tumor burden and reduced tumor volume in shID8 cell generated tumors (Fig. 5*a*). In marked contrast, D-4F treatment was ineffective in shSOD2ID8 cell generated tumors (Fig. 5*b*).

Discussion

We recently reported that apoA-I mimetic peptides inhibit tumor development in a mouse model of ovarian cancer.[5] In the our study, we investigated the mechanism by which apoA-I mimetic peptides inhibit tumor development. The current working model for the mechanism of action of apoA-I mimetic peptides is their ability to bind[15] and remove[16] oxidized lipids and thereby to inhibit inflammatory responses. Previous studies have demonstrated that the overall oxidant status, especially in lipoproteins, is altered from being pro-oxidative to one that is antioxidative after apoA-I mimetic peptide treatment.[19–22] Reactive oxygen species (ROS) are produced during cellular metabolism and also participate as important mediators of signal transduction pathways. It is known that ROS may serve as messengers in cellular signaling transduction pathways, and that a moderate increase of certain ROS such as superoxide and hydrogen peroxide may promote cellular growth and proliferation, and may contribute to cancer development.[23–26]

Our results demonstrate that D-4F decreases viability and inhibits proliferation in ID8 cells (Fig. 1). It is possible that the changes in viability were due to necrosis, apoptosis and autophagy; however, we show that the activities of LDH (necrosis), caspase 3 (apoptosis) and MDC (autophagy) were not altered by D-4F treatment in ID8 cells (Supporting Information Fig. 1). We conclude that the D4-F-mediated decrease in viability is mostly due to inhibition of proliferation of ID8 cells.

We examined whether apoA-I mimetic peptides exert their antiproliferative effects by modulating oxidative status of ID8 cells. Our results demonstrate that D-4F treatment reduces proliferation and viability of ID8 cells with concomitant improvement of the antioxidant status as measured by lipid peroxidation, protein carbonyl content, superoxide levels and H_2O_2 levels (Figs. 2*a*–2*d*). We also observed that GSH concentration in D-4F treated ID8 cells are significantly increased when compared to the untreated ID8 cells (data not shown). In further agreement with these findings, GSH and GSSG ratios, which are commonly used as markers for oxidative stress, were increased in D-4F treated ID8 cells (Fig. 2*e*).

Turkseven *et al.*[27] demonstrated that D-4F increases the levels of carbon monoxide and bilirubin as well as endothelial nitric oxide synthesis in endothelial progenitor cells in diabetic rats. These authors suggested that D-4F may have a clinically relevant role in reducing pro-atherogenic ox-LDL in diabetic rats. Kruger *et al.*[19] showed that D-4F induces hemeoxygenase-1 and extracellular superoxide dismutase, decreases endothelial cell sloughing, and improves vascular activity in a rat model of diabetes. MnSOD is a tumor suppressor protein that increases the dismutation rate of superoxide anion to hydrogen peroxide and inhibits cancer cell growth *in vitro* and *in vivo*.[28] Furthermore, many reports suggest that it could be a potential candidate for cancer gene therapy.[29,30] Our results

demonstrate that intracellular MnSOD expression is selectively upregulated by D-4F in ovarian cancer cells. Moreover, the increased MnSOD expression (Fig. 3) is reflected in enzyme activity and also a consistent decrease in the levels of O_2^- and in changes in lipid peroxidation and GSH/GSSG levels (Fig. 2).

The SODs are thought to be necessary for life in oxygen utilizing cells.[31] Knocking out the MnSOD gene in mice is lethal, with death occurring days after birth.[32] Knocking out the CuZnSOD gene in mice leads to increased susceptibility to oxidative stress.[33] Thus, normal cells and organisms need adequate amounts of SOD to protect against the toxicity from superoxide radicals. The tumor cells *in vivo* are under self-inflicted (and/or host inflicted) oxidative stress, and that stress contributes to malignancy. Therefore the antioxidants that really do act to decrease oxidative damage *in vivo* might have anticancer effects.[34] Enzyme activity is a more important parameter to determine the function of MnSOD because the expression of MnSOD mRNA may not necessarily mean an increase in MnSOD protein.[35] Therefore, we specifically studied enzymatic activity of MnSOD, and our results suggest that treatment of D-4F in ID8 cells significantly decreases the proliferation, which in turn coincides with increased activity of MnSOD.

Our results establish a direct correlation between the reduction of ROS levels and the inhibition of proliferation in ID8 cells. Antioxidant enzymes exhibit synergistic interactions by protecting each other from specific free radical attacks,[36,37] and they have the capacity to lower the free radical burden and neutralize excess free radicals due to oxidative stress conditions. Antioxidant enzymes serve as catalysts that can act at one or more of the three stages of free radical formation: initiation, propagation and termination. Therefore, it is possible that antioxidant enzymes can prevent cellular and tissue damage in the human body. The mechanism of induction of MnSOD by D-4F is not known and will need to be determined. To determine whether D-4F caused these changes by acting internally or externally to the cell, we treated ID8 cells with ^{14}C-labeled 4F and counted both the cytosol and mitochondrial fractions for radioactivity. We did not see any accumulation of the peptide in the cellular compartments after 24 hrs of treatment (Supporting Information Fig. 2) suggesting that apoA-I mimetic peptides exert their antitumorigenic effects from the outside.

A natural supposition, given 4F's affinity for oxidized lipids, is that D-4F is binding lipids present in the media or on the surface of the cells that are acting as signaling molecules, whose binding and potential sequestration then produces the changes we observed. It was recently reported that apoA-I and apoA-I mimetic peptides bind LPA (a pro-inflammatory lysophospholipid), but that the apoA-I mimetic peptides bind LPA with an affinity that is six orders of magnitude greater than apoA-I. We recently reported that serum LPA level (between 0.1 and 0.4 μM in control mice) was significantly reduced in mice that received apoA-1 mimetic peptides when compared to ID8 cell induced control mice.[5] Thus it is possible that the increase in MnSOD expression in D-4F treated ID8 cells is due to removal of LPA by D-4F. To test this directly, we treated ID8 cells with LPA and determined the expression of MnSOD. We observed that LPA does not affect MnSOD expression in ID8 cells either with or without D-4F treatment (Supporting Information Fig. 3), suggesting that removal of LPA may not be a direct mechanism in MnSOD induction by D-4F. Since apoA-I mimetic peptides bind to a number of pro-inflammatory lipids with remarkable affinity, we suggest that oxidized lipids, other than LPA, may be responsible for MnSOD levels in ID8 cells.

Our *in vivo* results (Fig. 5) showed that MnSOD expression in ID8 cells is necessary for the antitumorigenic effects of D-4F. Interestingly, we observed that the tumors generated from shSOD2ID8 cell injections were smaller (although not significant) from those in the shID8

cell injections (Fig. 5). The differences in tumor sizes may be due to the differences in the ability of the two cell lines to grow *in vivo*. Alternatively, although less likely, it is possible that basal MnSOD activity is required for the growth of ID8 cells *in vivo*. Further studies are needed to clarify this issue.

In conclusion, our *in vitro* (Fig. 4) and *in vivo* (Fig. 5) data strongly support a role for MnSOD in D-4F mediated inhibition of cell proliferation and tumor development. We propose that D-4F treatment acts as a barrier for tumor development by acting as an antioxidant. Antioxidants are notable for boosting the immune system because immune system could be modulated both by ROS levels and antioxidants. In line with these results, we recently reported that L-5F, another apoA-I mimetic peptide, affects tumor angiogenesis.[18] We postulate that D-4F and other apoA-I mimetic peptides may be utilized as novel therapies for the treatment of diseases that are regulated by pro-oxidant processes, including cardiovascular diseases and cancer. Future studies will determine the exact nature of D-4F mediated MnSOD induction.

Acknowledgments

The authors thank Dr. Gautam Chaudhuri and Dr. Sen Suvajit (Dept. of OB/GYN, UCLA) for kindly providing the DHE dye to measure superoxide radicals and further technical supports for this article. R.F.E. received the VA Merit I Award and the Wendy Stark Foundation and Sue and Mel Geleibter Family Foundation USPHS grants HL-30568 (A.M.F., M.N., S.T.R. and V.G.) and HL-082823 (S.T.R.).

Abbreviations

Apo A-I	apolipoprotein A-I
DHE	dihydroethidium
EOC	epithelial ovarian cancer
GSH	reduced glutathione
H_2O_2	hydrogen peroxide
KRPG	Krebs–ringer phosphate glucose buffer
LPO	lipid peroxidation
MDA	malondialdehyde
O_2^-	superoxide
ROS	reactive oxygen species

References

1. Kim D, Hoory T, Monie A, Wu A, Hsueh WT, Pai SI, Hung CF. Delivery of chemotherapeutic agents using drug-loaded irradiated tumor cells to treat murine ovarian tumors. J Biomed Sci. 2010; 17:61. [PubMed: 20659328]
2. Kozak KR, Amneus MW, Pusey SM, Su F, Luong MN, Luong SA, Reddy ST, Farias-Eisner R. Identification of biomarkers for ovarian cancer using strong anion-exchange ProteinChips: potential use in diagnosis and prognosis. Proc Natl Acad Sci USA. 2003; 100:12343–8. [PubMed: 14523236]
3. Kozak KR, Su F, Whitelegge JP, Faull K, Reddy S, Farias-Eisner R. Characterization of serum biomarkers for detection of early stage ovarian cancer. Proteomics. 2005; 5:4589–96. [PubMed: 16237736]
4. Su F, Lang J, Kumar A, Ng C, Hsieh B, Suchard MA, Reddy ST, Farias-Eisner R. Validation of candidate serum ovarian cancer biomarkers for early detection. Biomark Insights. 2007; 2:369–75. [PubMed: 19662218]

5. Su F, Kozak KR, Imaizumi S, Gao F, Amneus MW, Grijalva V, Ng C, Wagner A, Houg G, Farias-Eisner G, Anantharamaiah GM, Van Lenten BJ, et al. ApoA-I and apoA-I mimetic peptides inhibit tumor development in a mouse model of ovarian cancer. Proc Natl Acad Sci USA. 2010; 107:19997–20002. [PubMed: 21041624]
6. Van Lenten BJ, Navab M, Anantharamaiah GM, Buga GM, Reddy ST, Fogelman AM. Multiple indications for anti-inflammatory apolipoprotein mimetic peptides. Curr Opin Investig Drugs. 2008; 9:1157–62.
7. Navab M, Anantharamaiah GM, Reddy ST, Van Lenten BJ, Fogelman AM. Apo A-1 mimetic peptides as atheroprotective agents in murine models. Curr Drug Targets. 2008; 9:204–9. [PubMed: 18336238]
8. Bloedon LT, Dunbar R, Duffy D, Pinell-Salles P, Norris R, DeGroot BJ, Movva R, Navab M, Fogelman AM, Rader DJ. Safety, pharmacokinetics, and pharmacodynamics of oral apoA-I mimetic peptide D-4F in high-risk cardiovascular patients. J Lipid Res. 2008; 49:1344–52. [PubMed: 18323573]
9. Sherman CB, Peterson SJ, Frishman WH. Apolipoprotein A-I mimetic peptides: a potential new therapy for the prevention of atherosclerosis. Cardiol Rev. 2010; 18:141–7. [PubMed: 20395699]
10. Horiuchi A, Itoh K, Shimizu M, Nakai I, Yamazaki T, Kimura K, Suzuki A, Shiozawa I, Ueda N, Konishi I. Toward understanding the natural history of ovarian carcinoma development: a clinicopathological approach. Gynecol Oncol. 2003; 88:309–17. [PubMed: 12648580]
11. Delimaris I, Faviou E, Antonakos G, Stathopoulou E, Zachari A, Dionyssiou-Asteriou A. Oxidized LDL, serum oxidizability and serum lipid levels in patients with breast or ovarian cancer. Clin Biochem. 2007; 40:1129–34. [PubMed: 17673194]
12. Valko M, Rhodes CJ, Moncol J, Izakovic M, Mazur M. Free radicals, metals and antioxidants in oxidative stress-induced cancer. Chem Bio Interact. 2006; 160:1–40. [PubMed: 16430879]
13. Dreher D, Junod AF. Role of oxygen free radicals in cancer development. Eur J Cancer. 1996; 32A:30–8. [PubMed: 8695238]
14. Ou Z, Ou J, Ackerman AW, Oldham KT, Pritchard KA Jr. L-4F, an apolipoprotein A-1 mimetic, restores nitric oxide and superoxide anion balance in low-density lipoprotein-treated endothelial cells. Circulation. 2003; 107:1520–24. [PubMed: 12654610]
15. Van Lenten BJ, Wagner AC, Anantharamaiah GM, Navab M, Reddy ST, Buga GM, Fogelman AM. Apolipoprotein A-I mimetic peptides. Curr Atheroscler Rep. 2009; 11:52–7. [PubMed: 19080728]
16. Imaizumi S, Grijalva V, Navab M, Van Lenten BJ, Wagner AC, Anantharamiah GM, Fogelman AM, Reddy ST. L-4F differentially alters plasma levels of oxidized fatty acids resulting in more anti-inflammatory HDL in mice. Drug Metab Lett. 201(4):139–48.
17. Zhao H, Kalivendi S, Zhang H, Joseph J, Nithipatikom K, Vásquez-Vivar J, Kalyanaraman B. Superoxide reacts with hydroethidine but forms a fluorescent product that is distinctly different from ethidium: potential implications in intracellular fluorescence detection of superoxide. Free Radic Biol Med. 2003; 34:1359–68. [PubMed: 12757846]
18. Gao F, Vasquez SX, Su F, Roberts S, Shah N, Grijalva V, et al. L-5F, an apolipoprotein A-I mimetic peptide, inhibits tumor angiogenesis by suppressing activation of vascular endothelial growth factor/fibroblast growth factor signaling pathways. Integr Biol (Camb). 2011; 3:479–89. [PubMed: 21283904]
19. Kruger AL, Peterson S, Turkseven S, Kaminski PM, Zhang FF, Quan S, Wolin MS, Abraham NG. D-4F induces heme oxygenase-1 and extracellular superoxide dismutase, decreases endothelial cell sloughing, and improves vascular reactivity in rat model of diabetes. Circulation. 2005; 111:3126–34. [PubMed: 15939814]
20. Nguyen SD, Jeong TS, Sok DE. Apolipoprotein A-I-mimetic peptides with antioxidant actions. Arch Biochem Biophys. 2006; 451:34–42. [PubMed: 16759634]
21. Peterson SJ, Husney D, Kruger AL, Olszanecki R, Ricci F, Rodella LF, Stacchiotti A, Rezzani R, McClung JA, Aronow WS, Ikehara S, Abraham NG. Long-term treatment with the Apolipoprotein A1 mimetic peptide increases antioxidants and vascular repair in type I diabetic rats. J Pharmacol Exp Ther. 2007; 322:514–20. [PubMed: 17488882]

22. Vaziri ND, Kim HJ, Moradi H, Farmand F, Navab K, Navab M, Hama S, Fogelman AM, Quiroz Y, Rodriguez-Iturbe B. Amelioration of nephropathy with apoA-1 mimetic peptide in apoE-deficient mice. Nephrol Dial Transplant. 2010; 25:3525–34. [PubMed: 20488818]

23. Burdon RH. Superoxide and hydrogen peroxide in relation to mammalian cell proliferation. Free Radic Biol Med. 1995; 18:775–794. [PubMed: 7750801]

24. Dorward A, Sweet S, Moorehead R, Singh G. Mitochondrial contributions to cancer cell physiology: redox balance, cell cycle, and drug resistance. J Bioenerg Biomembr. 1997; 29:385–92. [PubMed: 9387099]

25. Schimmel M, Bauer G. Proapoptotic and redox state-related signaling of reactive oxygen species generated by transformed fibroblasts. Oncogene. 2002; 21:5886–96. [PubMed: 12185588]

26. Behrend L, Henderson G, Zwacka RM. Reactive oxygen species in oncogenic transformation. Biochem Soc Trans. 2003; 31:1441–4. [PubMed: 14641084]

27. Turkseven S, Kruger A, Mingone CJ, Kaminski P, Inaba M, Rodella LF, Ikehara S, Wolin MS, Abraham NG. Antioxidant mechanism of heme oxygenase-1 involves an increase in superoxide dismutase and catalase in experimental diabetes. Am J Physiol Heart Circ Physiol. 2005; 289:H701–07. [PubMed: 15821039]

28. Weydert CJ, Waugh TA, Ritchie JM, Iyer KS, Smith JL, Li L, Spitz DR, Oberley LW. Overexpression of manganese or copper-zinc superoxide dismutase inhibits breast cancer growth. Free Radic Biol Med. 2006; 41:226–37. [PubMed: 16814103]

29. Weydert CJ, Zhang Y, Sun W, Waugh TA, Teoh ML, Andringa KK, Aykin-Burns N, Spitz DR, Smith BJ, Oberley LW. Increased oxidative stress created by adenoviral MnSOD or CuZnSOD plus BCNU (1,3-bis (2-chloroethyl)-1-nitrosourea) inhibits breast cancer cell growth. Free Radic Biol Med. 2008; 44:856–67. [PubMed: 18155673]

30. Oberley LW. Mechanism of the tumor suppressive effect of MnSOD overexpression. Biomed Pharmacother. 2005; 59:143–148. [PubMed: 15862707]

31. Yuping Z, Smith BJ, Oberley LW. Enzymatic activity is necessary for the tumor-suppressive effects of MnSOD. Antioxid Redox Signal. 2006; 8:1283–93. [PubMed: 16910776]

32. Lebovitz RM, Zhang H, Vogel H, Cartwright J Jr, Dionne L, Lu N, Huang S, Matzuk MM. Neurodegeneration, myocardial injury, and perinatal death in mitochondrial superoxide dismutase-deficient mice. Proc Natl Acad Sci USA. 1996; 93:9782–87. [PubMed: 8790408]

33. Kondo T, Reaume AG, Huang TT, Murakami K, Carlson E, Chen S, Scott RW, Epstein CJ, Chan PH. Edema formation exacerbates neurological and histological outcomes after focal cerebral ischemia in CuZn-superoxide dismutase knockout mutant mice. Acta Neurochir Suppl. 1997; 70:62–64. [PubMed: 9416279]

34. Halliwell B. Oxidative stress and cancer: have we moved forward? Biochem J. 2007; 401:1–11. [PubMed: 17150040]

35. Czaja MJ, Schilsky ML, Xu Y, Schmiedeberg P, Compton A, Ridnour L, Oberley LW. Induction of MnSOD gene expression in a hepatic model of TNF-α toxicity does not result in increased protein. Am J Physiol. 1994; 266:G737–44. [PubMed: 8179009]

36. Blum J, Fridovich I. Inactivation of glutathione peroxidase by superoxide radical. Arch Biochem Biophys. 1985; 240:500–8. [PubMed: 2992378]

37. Wang SY, Lewers KS, Bowman L, Ding M. Antioxidant activities and anticancer cell proliferation properties of wild strawberrie. J Am Soc Hort Sci. 2007; 132:647–658.

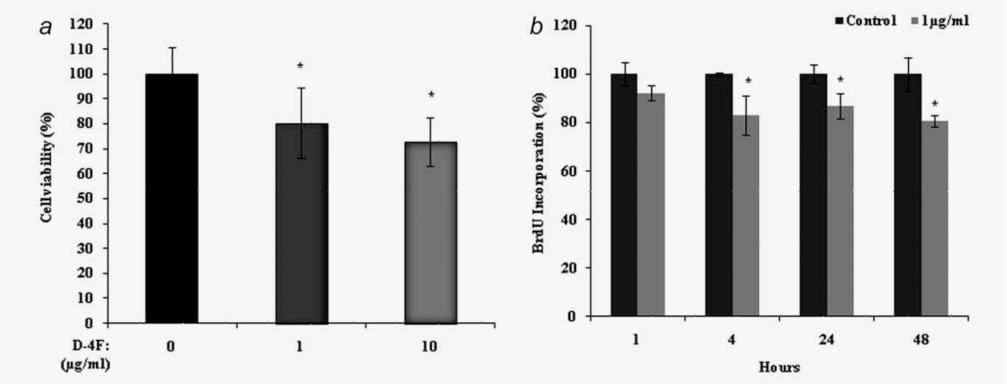

Figure 1.

Inhibition of cell viability and proliferation by D-4F. ID8 cells were seeded at 2×10^3 cells per well and treated with the indicated concentrations of D-4F for 24 hrs as described under "Materials and Methods" section. (*a*). Cell viability was assessed by CellTiter 96® AQueous nonradioactive cell proliferation assay (MTS). The percentage of live cells was determined as described under Materials and Methods. The values represent the mean ± SD of triplicates from three independent experiments ($n = 3$), $*p < 0.05$ *vs.* control ID8 cells. (*b*). Cell proliferation of ID8 cells was determined by measuring the incorporation of BrdU by treatment of cells with the D-4F. The figure represents the percentage of BrdU absorbance in D-4F treated and untreated ID8 cells. Values were expressed as percentage ($n = 3$), $*p < 0.05$ *vs.* control ID8 cells.

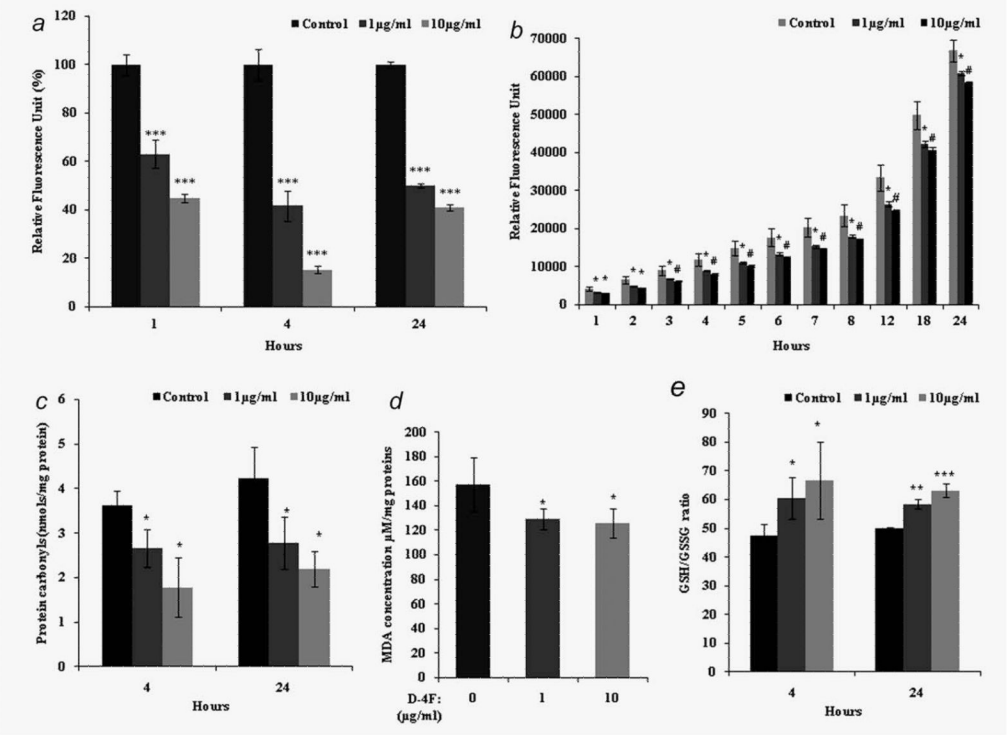

Figure 2.

D-4F reduces cellular oxidative stress in ID8 cells. (*a*). Superoxide levels were measured with DHE. ID8 cells (1×10^6) were seeded in six well plates. Experiments were performed with or without D-4F (1 or 10 μg/ml) for 1, 4 and 24 hrs and all groups were incubated with dihydroethidium (10 μM) for 30 min. The florescence was measured using BMG fluorescence spectrometer. Values were expressed as percentage ($n = 3$), ***$p < 0.001$ *vs.* control ID8 cells. (*b*). Hydrogen peroxide levels were measured by using amplex red. ID8 cells were treated with or without D-4F (1 or 10 μg/ml) and the rate of total cellular H_2O_2 production was measured using the amplex red dye with 5 units/mL HRP. Fluorescence measurements were monitored every 1 hr at 37°C at 563 nm excitation and 585 nm emission. Values on the Y-axis represent relative fluorescence units *$p < 0.05$, $^{\#}p < 0.01$ *vs.* control ID8 cells. (*c*). Protein carbonyls (nmol/mg proteins) were determined by using a kit from Cayman Chemicals (Ann Arbor, MI). ID8 cells were treated with D-4F (1 or 10 μg/ml) at 4 and 24 hrs. Data were represented as mean ± SD, *$p < 0.05$ *vs.* control ID8 cells. (*d*). Lipid peroxidation was determined by thiobarbituric acid reactive substances (TBARS) using Cayman chemical assay kit. ID8 cells (1×10^6) were harvested and assayed as per manufacturer protocol. Data were shown as mean ± S.D, *$p < 0.05$ *vs.* control ID8 cells. (*e*). GSH/GSSG ratios were determined using a Cayman chemical assay kit. ID8 cells (1×10^6) were treated with or without D-4F (1 or 10 μg/ml) for 24 hrs. After being harvested, cells were lyses with 50 mM phosphate buffer and assayed as per manufacturer's protocol as mentioned under Materials and Methods. Data were shown as mean ± S.D, *$p < 0.05$, **$p < 0.01$, ***$p < 0.001$ *vs.* control ID8 cells.

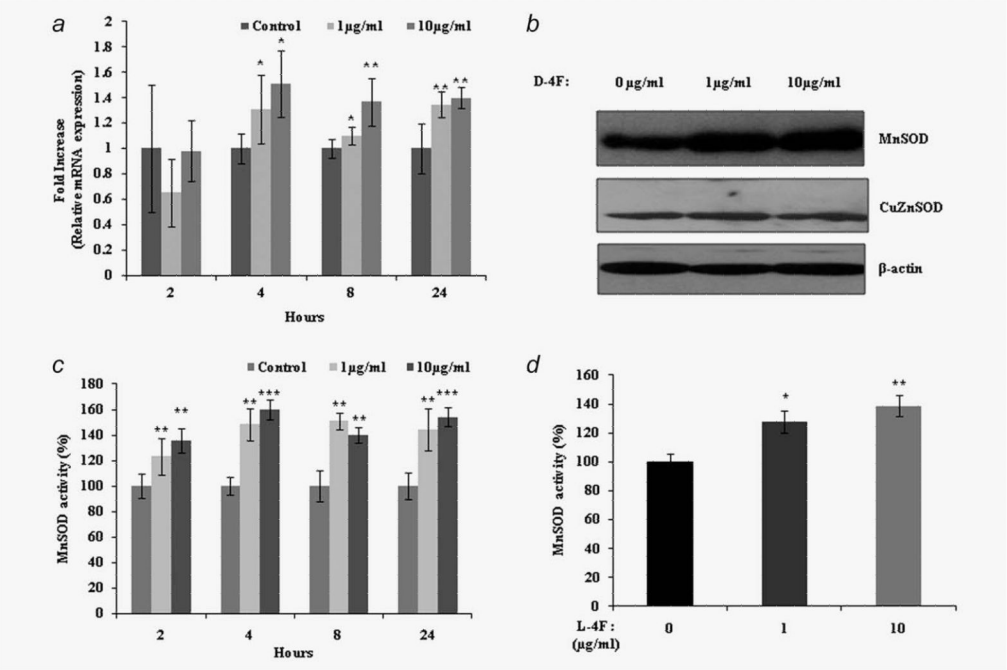

Figure 3.

D-4F treatment increases MnSOD expression and activity in ID8 cells. MnSOD message, protein and activity were determined from D-4F (1 or 10 μg/ml) treated and untreated ID8 cells at 24 hrs. (*a*) Levels of MnSOD mRNA were measured using qRT-PCR. Relative MnSOD mRNA fold expression was normalized with cyclophilin. Data were shown as fold increase, $*p < 0.05$. $**p < 0.01$ *vs.* control ID8 cells. (*b*) MnSOD and CuZnSOD protein expression. Total cell lysates were subjected to SDS-PAGE and transferred to nitrocellulose membranes. Blots were probed with antibodies against MnSOD, CuZnSOD and β-actin (loading control). (*c, d*). Specific activity of MnSOD in D-4F and L-4F treated cells. Cell pellets were homogenized in ice-cold phosphate buffer and enzymatic activity were measured using Cayman chemicals SOD assay kit. KCN (1 mM) were used for inhibition of CuZnSOD. Data were normalized to mg of protein of whole cell homogenates. The results are expressed as percentage of specific activity and represent the mean ± S.D, $*p < 0.05$, $**p < 0.01$, $***p < 0.001$ *vs.* control ID8 cells.

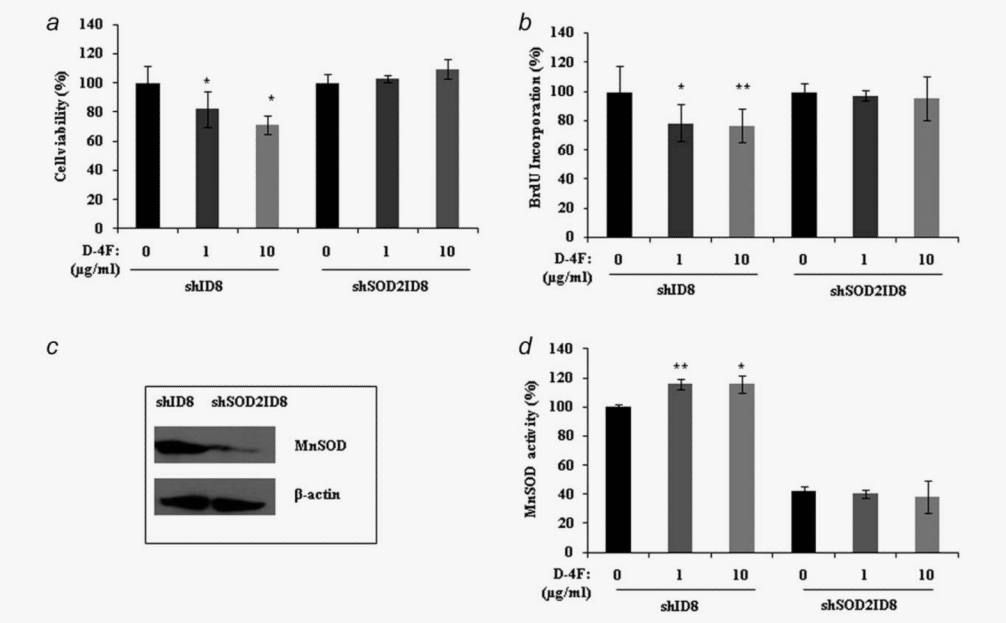

Figure 4.

D-4F-mediated inhibition of shID8/shSOD2ID8 cell proliferation requires the activity of MnSOD. (*a*) The shID8 and shSOD2ID8 were treated with D-4F for 24 hrs and cell viability was assessed by CellTiter 96® AQueous nonradioactive cell proliferation assay (MTS). (*b*) Cell proliferation of shID8 and shSOD2ID8 cells was determined by measuring the incorporation of BrdU by treatment of cells with the D-4F at 48 hrs. The results were shown as percentage by setting the control/untreated cell values to 100%, *$p < 0.05$, **$p < 0.01$ *vs.* control shID8 cells. (*c*) Lentiviral-mediated expression of a small hairpin RNAi motif directed against MnSOD shows silencing of MnSOD expression in western blot analyses in ID8 cells. The β-actin signal demonstrates equal loading. (*d*). Specific activity of MnSOD in D-4F treated shID8 and shSOD2ID8 cells. Cell pellets were homogenized in ice-cold phosphate buffer and enzymatic activity were measured using Cayman Chemicals SOD assay kit. KCN (1 mM) were used for inhibition of CuZnSOD. The results are expressed as percentage of specific activity and represent the mean ± S.D, *$p < 0.05$, **$p < 0.01$ *vs.* control.

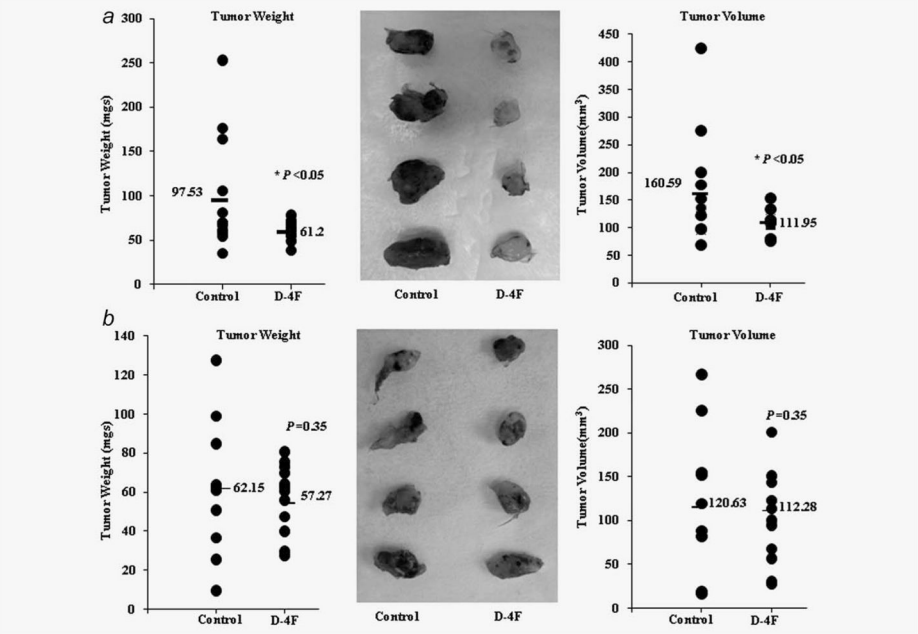

Figure 5.

In vivo study of the effect of D-4F on flank tumors generated using shID8 and shSOD2ID8 cells. (*a*) shID8 (5×10^6) cells were injected subcutaneously into the right flank of C57BL/6J mice ($n = 30$). Mice were randomly divided into two groups ($n = 15$), control and D-4F (300 μg/ml) treatment, respectively. Tumor weight and volume were measured after 5 weeks. Data represented significant reduction of tumor weight (*$p < 0.05$ *vs*. control) and tumor volume (*$p < 0.05$ *vs*.. control). Data were analyzed by student's *t*-test (one-tailed) on excel program for significant. (*b*). shSOD2ID8 (5×10^6) cells were injected subcutaneously into the right flank of C57BL/6J mice ($n = 15$ per treatment group). Mice were randomly divided into two groups ($n = 15$), control and D-4F treatment, respectively. Tumor weight and volume were measured after 5 weeks. Data were analyzed as above.